

Supramolecular Chemistry

Construction of Alkynylplatinum(II) Bzimpy-Functionalized Metallacycles and Their Hierarchical Self-Assembly Behavior in Solution Promoted by Pt...Pt and π - π Interactions**

Bo Jiang,^[a] Jing Zhang,^[a] Wei Zheng,^[a] Li-Jun Chen,^[a] Guang-Qiang Yin,^[a] Yu-Xuan Wang,^[a] Bin Sun,^[a] Xiaopeng Li,^[b] and Hai-Bo Yang*^[a]

Abstract: A family of new alkynylplatinum(II) 2,6-bis(benzimidazol-2'-yl)pyridine (bzimpy)-functionalized supramolecular metallacycles with different shapes and sizes have been successfully prepared by coordination-driven self-assembly. The obtained metallacycles showed switchable emission and a strong tendency to form intermolecular Pt...Pt and π - π stacking interactions in solution that were not displayed by their individual precursors. Further investigation revealed that the existence of the metallacyclic scaffold at the core

could facilitate the formation of intermolecular Pt...Pt and π - π stacking interactions of peripheral alkynylplatinum(II) bzimpy units. Moreover, the shapes and sizes of the metallacyclic scaffold have a significant influence on the hierarchical self-assembly behavior. Among the three metallacycles, hexagonal metallacycle **A**, with a relatively small size, could spontaneously self-assemble into an aromatic guest stimuli-responsive metallogel at room temperature without a heating-cooling process.

Introduction

During the past few decades, the power and versatility of molecular self-assembly has been well illustrated by numerous examples of the use of noncovalent interactions in the construction of complicated supramolecular assemblies.^[1,2] Of the various self-assembly protocols, coordination-driven self-assembly has evolved to be one of the most attractive topics within supramolecular chemistry and materials science because of their wide applications in the fields of catalysis, sensing, drug delivery, and so forth.^[3–5] However, many building blocks used in coordination-driven self-assembly are simple, fairly inert building blocks that are often aliphatic or aromatic in nature. Therefore, in many cases, the resultant metallacycles or metal-lacages are unfunctionalized, which thus hinders the in-depth investigation of their further applications. With the aim of constructing functional organometallic architectures with pre-designed shapes and sizes, recent research efforts have focused

on incorporating functionality into the final discrete assemblies.^[6–8]

Platinum(II) polypyridine complexes have received considerable attention during the past few decades due to their extensive applications in various fields, such as catalysis, organic light-emitting diodes (OLEDs), and vapochromic materials.^[9–11] Among them, alkynylplatinum(II) bzimpy (bzimpy = 2,6-bis(benzimidazol-2'-yl)pyridine) complexes, which were first reported by Yam et al. in 2008, represented an important class of platinum(II) complexes due to their intriguing spectroscopic and luminescence properties, as well as their tunable intermolecular Pt...Pt and π - π stacking interactions.^[12] Moreover, by taking advantage of the dynamic nature of intermolecular Pt...Pt and π - π stacking interactions of the alkynylplatinum(II) bzimpy moiety, some stimuli-responsive systems, which displayed interesting solvatochromic behavior^[12c] and unusual memory property,^[12e] have been explored. We have recently reported a new alkynylplatinum(II) bzimpy-functionalized supramolecular metallacycle that displayed vapochromic behavior in the solid state with high stability.^[13] Inspired by our previous progress on functionalized metallacycles^[7] and hierarchical self-assembly,^[8] we envisioned that the combination of coordination-driven self-assembly with Pt...Pt and π - π stacking interactions would endow the resulting metallacycles with interesting hierarchical self-assembly behavior in solution; thus allowing for the formation of novel smart functional materials.

Herein, we present the successful construction of a family of new alkynylplatinum(II) bzimpy-functionalized metallacycles with different shapes and sizes by coordination-driven self-assembly. Interestingly, these novel metallacycles displayed switchable emission in different cyclohexane/CH₂Cl₂ composi-

[a] B. Jiang, J. Zhang, W. Zheng, L.-J. Chen, G.-Q. Yin, Y.-X. Wang, B. Sun, Prof. Dr. H.-B. Yang
Shanghai Key Laboratory of Green Chemistry and Chemical Processes
School of Chemistry and Molecular Engineering
East China Normal University, 3663 N. Zhongshan Road
Shanghai 200062 (P.R. China)
E-mail: hbyang@chem.ecnu.edu.cn

[b] Prof. Dr. X. Li
Department of Chemistry and Biochemistry
Texas State University, San Marcos TX 78666 (USA)

[**] Bzimpy = 2,6-bis(benzimidazol-2'-yl)pyridine.

Supporting information for this article can be found under
<http://dx.doi.org/10.1002/chem.201601682>.

tions accompanied by the enhancement of intermolecular Pt···Pt and π ··· π stacking interactions. Further investigation revealed that the metallacyclic scaffold at the core played an important role in the formation of intermolecular Pt···Pt and π ··· π stacking interactions. More importantly, hexagonal metallacycle **A** could spontaneously self-assemble into the aromatic guest stimuli-responsive metalgel at room temperature without a heating–cooling process mainly driven by intermolecular Pt···Pt and π ··· π stacking interactions. It should be noted that the recognition of aromatic guests with high selectivity has been very challenging.^[14] To the best of our knowledge, this study provides the first example of visual discrimination of aromatic compounds by using metalgels.

Results and Discussion

The alkynylplatinum(II)-containing dipyridine donors **a** and **b** (Figure 1) were easily synthesized through the coupling reaction of complexes **5** or **8** with chloroplatinum(II) precursor **6** in the presence of Et₃N and a catalytic amount of copper(I) iodide in 48.3 and 27.2% yield, respectively (Schemes S1 and S2 in the Supporting Information). Notably, both building blocks **a** and **b** carry two binding sites for multiple noncova-

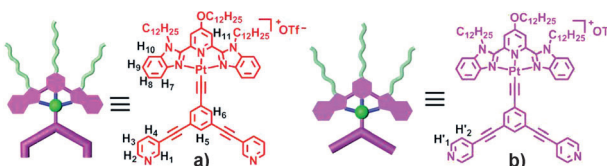
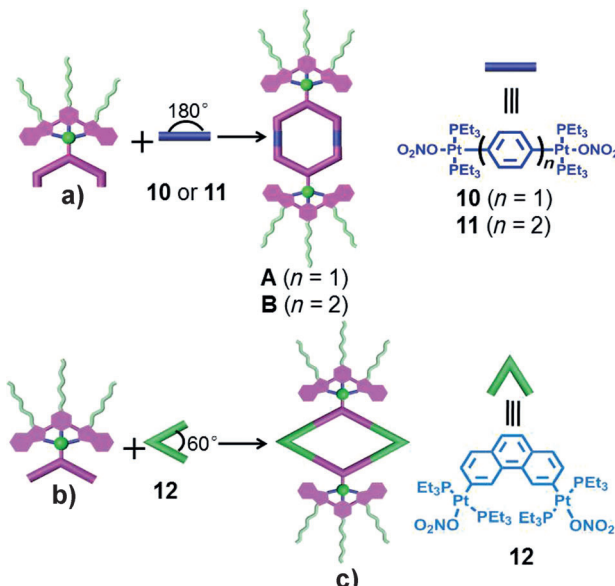


Figure 1. Molecular structures of alkynylplatinum(II)-containing dipyridine donors **a** and **b**.

lent interactions: the alkynylplatinum(II) bzimpy moiety has a strong tendency to form Pt···Pt and π ··· π stacking interactions and the pyridine can act as a donor unit to a variety of metal salts. Functionalized metallacycles **A–C**, containing two alkynylplatinum(II) bzimpy moieties, were prepared by simply mixing the donor ligands **a** or **b** with the corresponding diplatinum(II) acceptors **10–12** in a 1:1 ratio in a mixed solvent of acetone and water at 55 °C (Scheme 1). The di-Pt^{II} acceptors **10–12** exhibited different lengths and orientations, which allowed discrete metallacycles to be produced with different shapes and sizes. The PF₆[−] salts of these metallacycles were synthesized by dissolving the yellow NO₃[−] salt in acetone/H₂O and adding a saturated aqueous solution of KPF₆ to precipitate the products.

The structures of the obtained metallacycles were well characterized with multiple nuclear (¹H and ³¹P) NMR spectroscopy, which was consistent with the formation of discrete and highly symmetric species (Figures S1–S6 in the Supporting Information). For example, the ³¹P{¹H} NMR spectrum of **B** displayed a sharp singlet at δ = 13.97 ppm shifted upfield from the starting platinum acceptor **11** by approximately 5.09 ppm (Figure 2). Moreover, the protons of the pyridine rings exhibited clear downfield shifts (ca. H₁, 0.14 ppm; H₂, 0.05 ppm), which were caused by the loss of electron density upon coor-



Scheme 1. Self-assembly of dipyridyl donors **a** and **b** with the corresponding diplatinum(II) acceptors **10–12** into metallacycles **A–C** with different shapes and sizes.

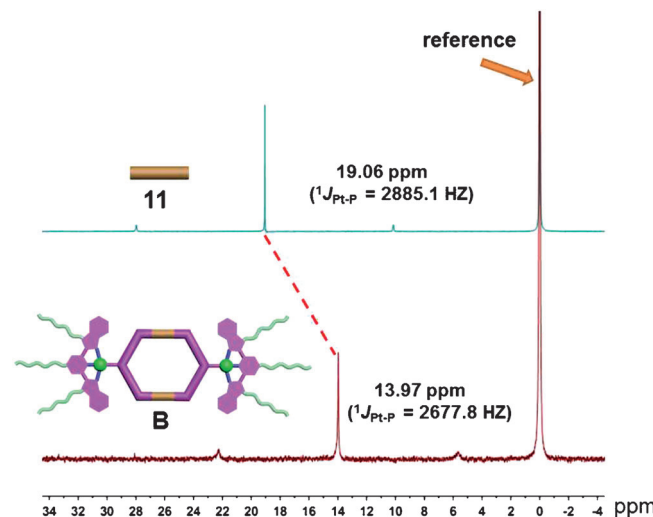


Figure 2. The ³¹P NMR spectra (161.9 MHz, 298 K) of acceptor **11** and metallacycle **B** in CD₂Cl₂.

dination of the pyridine-N atoms with the Pt^{II} metal center (Figure S3 in the Supporting Information). In addition, the structures of metallacycles **A–C** were further confirmed by ESI-TOF-MS, which allowed the assembly to remain intact to the maximum extent during the ionization process, while obtaining the high resolution required for isotopic distribution. For instance, the ESI-TOF-MS spectrum of **B** revealed three signals that corresponded to different charge states resulting from the loss of PF₆[−] counterions, [M–4PF₆]⁴⁺, [M–5PF₆]⁵⁺, and [M–6PF₆]⁶⁺, respectively, in which *M* represents the intact assembly (Figure 3a). Further investigation revealed that each isotope pattern of these signals was in good agreement with the corresponding simulated result. Similar results were ob-

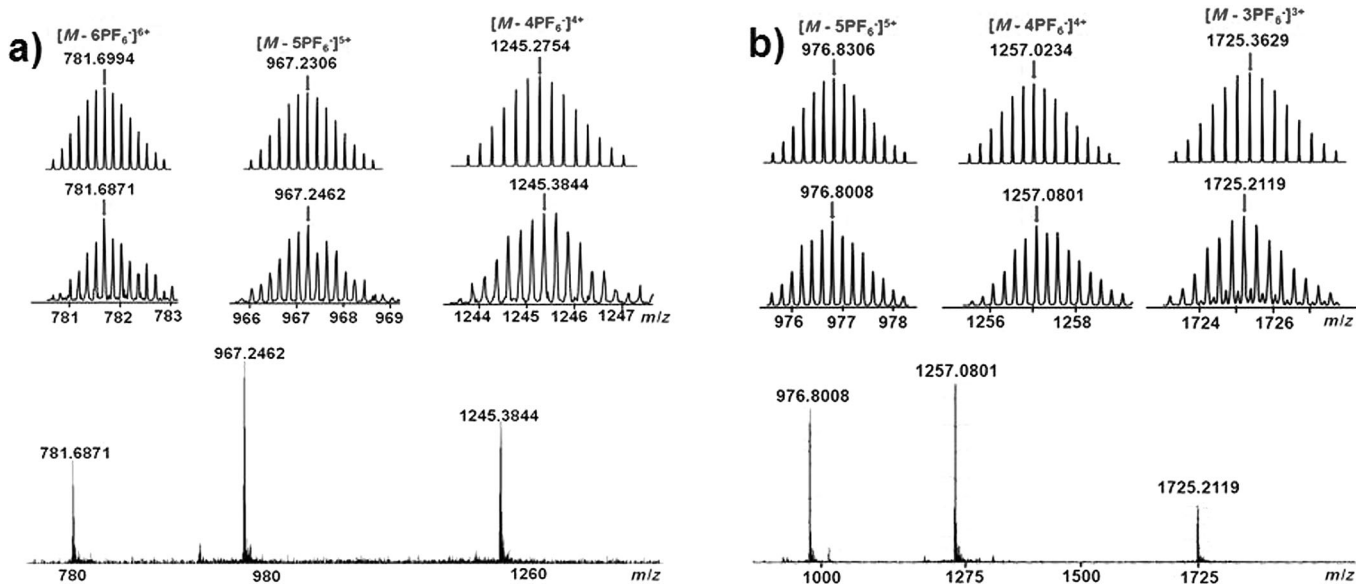


Figure 3. ESI-TOF-MS spectra of metallacycles **B** (a) and **C** (b). Inset: Theoretical (top) and experimental (bottom) isotopic distributions.

tained in the mass investigation of metallacycle **C** (Figure 3 b). Furthermore, diffusion-ordered NMR spectroscopy (DOSY) was employed to study the trend of size changes to metallacycles **A**, **B**, and **C**. As shown in Figures S26–S28 in the Supporting Information, a single band at $\log D = -9.45$, -9.59 , and -10.17 for metallacycles **A**, **B**, and **C**, respectively, were observed; these values indicated an appreciable size increase from metallacycle **A** to metallacycle **C**. All above data supported the highly efficient construction of alkynylplatinum(II)-functionalized metallacycles with well-defined shapes and sizes through coordination-driven self-assembly; thus avoiding time-consuming procedures and low yields often encountered in covalent synthesis protocols.

Dissolution of metallacycles **A–C** in CH_2Cl_2 gave pale-yellow solutions with similar UV/Vis absorption and emission spectra at room temperature (Figure S11 in the Supporting Information). The electronic absorption spectra of metallacycles **A–C** ($1.0 \times 10^{-5} \text{ M}$) showed intense intraligand (IL; $\pi \rightarrow \pi^*(\text{bzimpy})$) absorption bands at $\lambda = 295$ – 350 nm and relatively weak absorption bands at $\lambda = 400$ – 450 nm . The low-energy absorption bands are assigned as a metal-to-ligand charge-transfer (MLCT; $d\pi(\text{Pt}) \rightarrow \pi^*(\text{bzimpy})$) transition mixed with a ligand-to-ligand charge-transfer (LLCT; $\pi(\text{alkynyl}) \rightarrow \pi^*(\text{bzimpy})$) transition.^[12b] Upon photoexcitation at $\lambda = 420 \text{ nm}$, solutions of **A–C** in CH_2Cl_2 showed vibronic-structured triplet intraligand (${}^3\text{IL}$; $\pi \rightarrow \pi^*(\text{bzimpy})$) emissions at $\lambda_{\text{max}} = 551 \text{ nm}$; these emissions are attributed to the typical spectroscopic characteristic of monomeric platinum(II) bzimpy complexes.^[12c]

Furthermore, the UV/Vis absorption and emission spectra of functionalized metallacycles **A–C** ($1.0 \times 10^{-5} \text{ M}$) in different cyclohexane/ CH_2Cl_2 compositions were investigated. Metallacycle **A** was selected as a representative example to illustrate the absorption and emission changes. As shown in Figure 4a, the increase in the cyclohexane fraction from 0 to 70% led to a gradual decrease in intensity of the absorption band at $\lambda \approx 358 \text{ nm}$

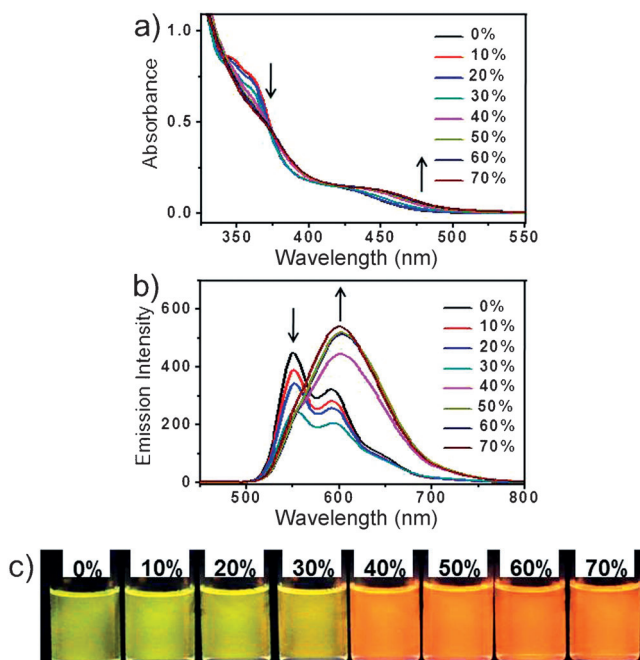


Figure 4. a) UV/Vis absorption and b) emission spectra **A** ($[\text{A}] = 1.0 \times 10^{-5} \text{ M}$) in CH_2Cl_2 with increasing cyclohexane content at 298 K. c) Photographs of **A** in mixtures of cyclohexane/ CH_2Cl_2 with different ratios under irradiation by a UV lamp at $\lambda = 365 \text{ nm}$.

with concomitant growth of an absorption tail at $\lambda \approx 500 \text{ nm}$ with a well-defined isosbestic point at $\lambda = 375 \text{ nm}$. Notably, the low-energy absorption tail at $\lambda \approx 500 \text{ nm}$ is usually assignable to a typical metal-metal-to-ligand charge-transfer (MMLCT) transition, which is related to intermolecular Pt...Pt and π – π stacking interactions.^[12c] Interestingly, with the addition of cyclohexane, the pale-yellow emission (100% CH_2Cl_2) gradually turned orange (70% cyclohexane) under irradiation by a UV

lamp at $\lambda=365$ nm (Figure 4c). Correspondingly, the emission spectra revealed that the emission at $\lambda_{\text{max}} \approx 551$ nm was gradually quenched upon increasing the cyclohexane fraction from 0 to 30% (Figure 4b). Upon further addition of cyclohexane, a significant redshift of the emission band (54 nm), accompanied by an enhancement in intensity, was observed. All of the aforementioned results suggested that the conversion of metallacycle **A** from the monomeric form to aggregates occurred mainly driven by Pt···Pt and π – π stacking interactions. Because metallacycle **A** is insoluble in cyclohexane, it is likely that it tends to aggregate as a result of reduced solvation. Similarly, metallacycles **B** and **C** also displayed clear absorption and emission changes in different cyclohexane/CH₂Cl₂ compositions (Figures S14–S16 in the Supporting Information).

Moreover, the ¹H NMR spectra of metallacycle **A** in different solvent compositions provided further support for the existence of π – π stacking interactions during the aggregation process (Figure S8 in the Supporting Information). In CD₂Cl₂, complex **A** showed well-resolved sharp signals with well-defined coupling patterns. Upon increasing the [D₁₂]cyclohexane content in CD₂Cl₂ at the same concentration, phenyl protons H₇ and H₁₀ shifted upfield, while pyridine protons H₁ and H₄ shifted downfield. At the same time, all aromatic signals gradually became very broad and poorly resolved NMR signals. Moreover, a higher [D₁₂]cyclohexane content in CD₂Cl₂ (40%) led to a very broad and almost featureless NMR spectrum, consistent with the corresponding UV/Vis absorption study, which indicated that metallacycle **A** could undergo self-assembly to form aggregate species.

Notably, neither donor ligand **a** nor **b** presented similar spectroscopic properties to those of metallacycles **A**–**C** under the same conditions. For example, the UV/Vis absorption spectrum of **a** ($[a]=1.0 \times 10^{-5}$ M) in various solvent compositions showed main absorption bands at $\lambda=288$, 349, and 430 nm, which was similar to that of the spectrum of a solution in pure CH₂Cl₂ (Figure S12a in the Supporting Information). It should be noted that the new absorption tail at $\lambda_{\text{max}} > 500$ nm was not observed, even though the cyclohexane fraction was up to 80%, which indicated that building block **a** could not form intermolecular Pt···Pt and π – π stacking interactions at this concentration. The corresponding emission study of **a** also supported the above conclusion. When the cyclohexane fraction was below 70% in mixed solvents, the high-energy emission band at $\lambda=550$ nm dropped in intensity accompanied by a blueshift in the emission maxima (Figure S12b in the Supporting Information), which was typical optic behavior of monomeric platinum(II) bzimpy complexes. All of the above results indicated that the existence of the metallacyclic scaffold at the core might facilitate the formation of intermolecular Pt···Pt and π – π stacking interactions of peripheral alkynylplatinum(II) bzimpy units in the mixed solvents; these interactions were not displayed by their individual components.

To prove such an assumption, further spectroscopic investigation of metallacycle **A** in a mixture of cyclohexane and CH₂Cl₂ (v/v, 2/5) was carried out to investigate the importance of the metallacyclic scaffold during the aggregation process. Interestingly, with the addition of tetrabutylammonium bro-

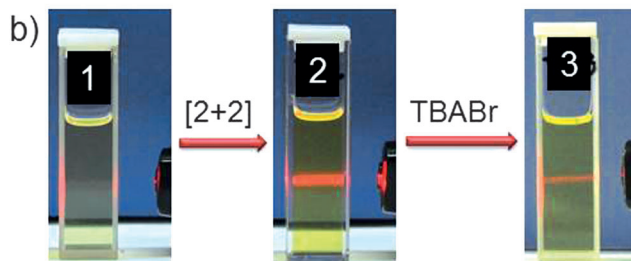
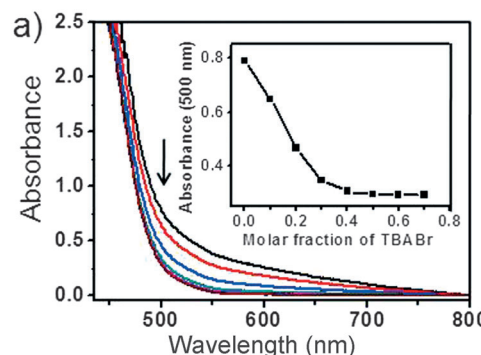


Figure 5. a) UV/Vis absorption spectra of metallacycle **A** ($[A]=2.5 \times 10^{-4}$ M) with the addition of TBABr. The inset shows plots of the absorbance at $\lambda=500$ nm for **A** versus the molar fraction of TBABr. b) Photographs of the Tyndall effect of ligand **a** (left), metallacycle **A** (middle), and metallacycle **A** after the addition of TBABr (6.0 equiv; right) in CH₂Cl₂/cyclohexane = 5:2.

mide (TBABr) to the solution of **A** ($[A]=2.5 \times 10^{-4}$ M), the UV/Vis absorption band at $\lambda_{\text{max}} > 500$ nm decreased remarkably (Figure 5a), which implied that intermolecular Pt···Pt and π – π stacking interactions gradually decayed upon the addition of Br[−]. Moreover, clear changes to the Tyndall effect were also observed in the mixture of cyclohexane and CH₂Cl₂ (v/v, 2/5). As shown in Figure 5b, the solution of **A** ($[A]=1.0 \times 10^{-4}$ M) displayed clear evidence of the Tyndall effect, whereas in the case of free ligand **a**, at the same concentration, this scattering phenomenon did not occur. These phenomena indicated that aggregates of **A** formed at this concentration. Notably, the Tyndall effect almost disappeared after the addition of TBABr (6.0 equiv), which suggested that the aggregate species was destroyed. Such stimuli-responsive behavior was attributed to the halide-induced disassembly of the metallacycle, which was well illustrated by *in situ* multinuclear NMR (¹H and ³¹P) spectroscopy experiments with **A** in CD₂Cl₂. As shown in Figure S18 in the Supporting Information, after the addition of TBABr (4.0 equiv) to the solution of **A** (2.5 mM) in CD₂Cl₂, typical proton signals of metallacycle **A** disappeared and signals assigned to free ligand **a** were found in the ¹H NMR spectrum; this indicated the complete disassembly of the metallacyclic scaffold at the core. In addition, the increase in coupling of flanking ¹⁹⁵Pt satellites ($\approx \Delta J(P,\text{Pt}) = 96.5$ Hz) was observed; this was in agreement with the formation of the new Pt–Br complex **13** (Figure S19 in the Supporting Information). Such NMR spectroscopy experiments provided direct evidence for the halide-induced disassembly of supramolecular metallacycle **A**. This observation provided further proof for the importance

of the metallacyclic scaffold in the formation of intermolecular Pt^{..}Pt and π - π stacking interactions in this study.

Interestingly, functionalized metallacycle **A** could form a yellow, translucent metallogel in a mixture of cyclohexane and CH₂Cl₂ (v/v, 2/5) when the concentration was increased to 1.3 mM. The critical gelation concentration (CGC) was determined to be 7.2 mg mL⁻¹. Moreover, the formation of such a metallogel was observed 2 h after the compound was dissolved in the solvent mixture at room temperature without heating, which is significantly different from most known supramolecular gels, which usually require a heating–cooling process.^[15] The generation of metallogel **A** was further confirmed by rheology investigations at 25 °C. As shown in Figure 6, the storage modulus (G') was higher than the loss

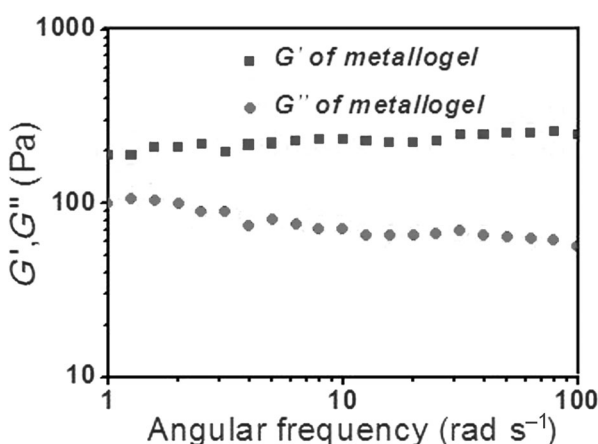


Figure 6. Rheological characterization of metallogel **A** in 5:2 (v/v) CH₂Cl₂/cyclohexane.

modulus (G') in the higher-frequency region ($\omega > 1.0 \text{ rad s}^{-1}$); this is consistent with the typical characteristic of gels. Moreover, SEM images were recorded to study the morphologies of the obtained xerogel, in which a 3D network of fibrous structures was observed (Figure 7 b). Notably, ligand **a** was not able to form a stable gel under the same conditions, which again supported the important role of the metallacyclic scaffold during the aggregation process. Neither metallacycle **B** nor **C** formed a stable gel; this might be caused by the low solubility of **B** and weak intermolecular interactions of **C**.

Further investigation revealed that the obtained metallogel **A** was selectively responsive to the addition of coronene, which induced the transition from the gel to solution (Figure 7 a). For instance, when coronene (1.0 equiv) was added to the surface of metallogel **A**, the metallogel turned into a solution very quickly (in 1 min). However, other common aromatic organic compounds, such as pyrene, anthracene, 1-naphthol, tetraphenylethylene, and carbazole, could not induce such collapse of the gel even, if over 10.0 equivalents of organic guests were added. Notably, although a large number of stimuli-responsive supramolecular gels have been reported, examples of aromatic guest stimuli-responsive gels, which have potential

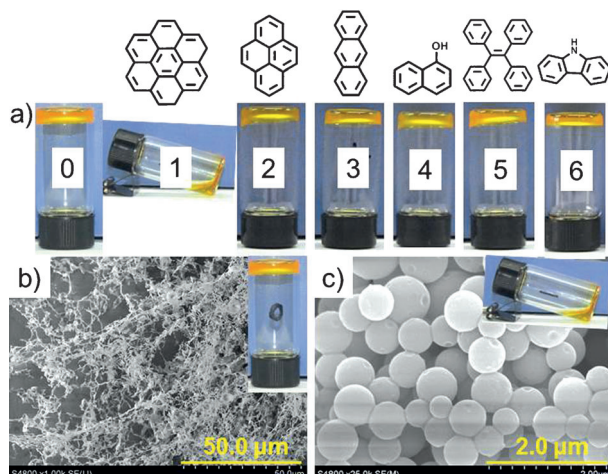


Figure 7. a) Photographs of metallogel **A** in a mixture of cyclohexane and CH₂Cl₂ (v/v, 2/5) after the addition of various aromatic organic compounds; from left to right: 0) no additive, 1) coronene (1.0 equiv), 2) pyrene (16.0 equiv), 3) anthracene (12.0 equiv), 4) 1-naphthol (19.0 equiv), 5) tetraphenylethylene (10.0 equiv), 6) carbazole (8.0 equiv). b) SEM image of the xerogel of **A**. c) SEM image of metallogel **A** after the addition of coronene (1.0 equiv).

applications in visual discrimination,^[16] have been relatively unexplored.

To understand the driving forces for the collapse of the metallogel induced by coronene, ¹H NMR spectroscopy studies were performed (Figure 8). With the addition of coronene into a solution of metallacycle **A** (3.0 mM) in CD₂Cl₂, pyridyl proton H₁₁ and phenyl proton H₇ shifted upfield from $\delta = 7.553$ to 6.198 ppm and $\delta = 8.578$ to 8.131 ppm, respectively; this is in agreement with the existence of strong π - π stacking interactions between the bzimpy moieties and coronene molecules. Moreover, a SEM investigation revealed that, after the addition of 1.0 equivalent of coronene, the morphology of the xerogel transformed into spherical structures, in sharp contrast to the fibrous structures of the original metallogel (Figure 7 c). Based on these experimental results, we proposed that the fibrous structures were first formed mainly through intermolecular

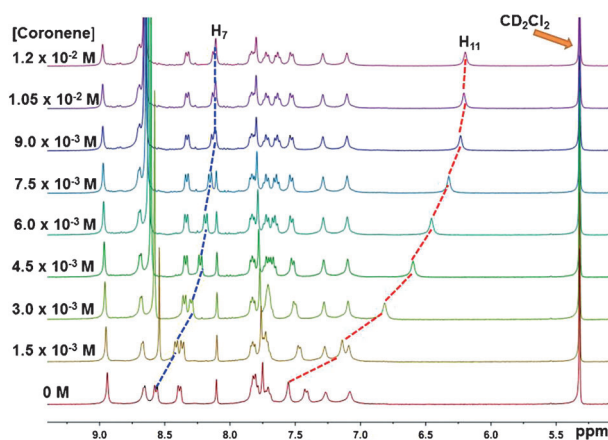
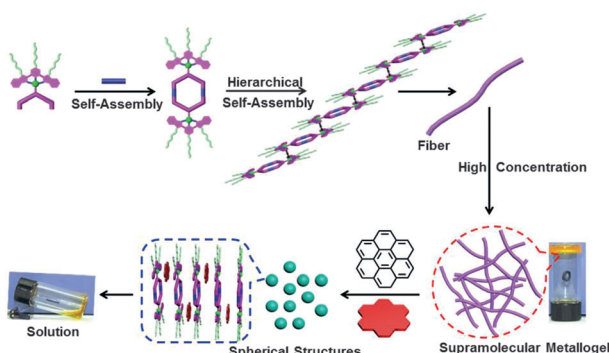


Figure 8. Partial ¹H NMR spectra of **A** ($[A] = 3.0 \text{ mM}$) in CD₂Cl₂ with the addition of coronene.

Pt···Pt and π ··· π stacking interactions. Then, with the increase in concentration, the network of fibrous structures was formed because of the cross-linking of fibers, which finally generated the stable supramolecular metallo-gel. However, the addition of coronene induced the disruption of intermolecular Pt···Pt and π ··· π stacking interactions because the guest could insert between two bzimpy moieties through π ··· π interactions; thus resulting in the collapse of metallo-gel (Scheme 2).



Scheme 2. Proposed process for the formation of a supramolecular metallo-gel and the guest-induced gel-to-sol transformation.

Furthermore, to obtain further insight into the possible reason for the selective visual recognition induced by coronene, additional ^1H NMR spectroscopy studies were performed by employing different guests, such as pyrene or anthracene. As shown in Figure S9 in the Supporting Information, with the addition of pyrene to a solution of metallacycle **A** (3.0 mM) in CD_2Cl_2 , pyridyl proton H_{11} and phenyl proton H_7 only shifted from $\delta = 7.55$ to 7.43 ppm and $\delta = 8.55$ to 8.57 ppm, respectively; this suggested weak π ··· π stacking interactions between the bzimpy moieties and pyrene molecules. Similarly, in the case of anthracene, almost no change to the proton signals was observed (Figure S10 in the Supporting Information), which indicated that there was no clear π ··· π stacking interactions between the bzimpy moieties and anthracene molecules. On the basis of the collected experimental results, we proposed that the π ··· π stacking interactions between the bzimpy moieties and other common aromatic organic compounds employed herein were too weak to disrupt intermolecular Pt···Pt and π ··· π stacking interactions. Thus, the metallo-gel remained untouched, even with the presence of excess aromatic organic compounds; this allowed selective visual recognition to occur.

Conclusion

A family of new alkynylplatinum(II) bzimpy functionalized supramolecular metallacycles with different shapes and sizes were successfully prepared with high efficiency through [2+2] coordination-driven self-assembly. Notably, the metallacyclic scaffold at the core facilitated the formation of intermolecular Pt···Pt and π ··· π stacking interactions of peripheral alkynylplatinum(II) bzimpy units, which allowed switchable emission, ranging from pale yellow to orange, in different cyclohexane/

CH_2Cl_2 compositions. Moreover, metallacycle **A** was able to hierarchically self-assemble into a stable supramolecular metallo-gel at room temperature without the need for a heating–cooling process. Further investigation revealed that the obtained metallo-gel was selectively responsive to coronene as an aromatic guest, which could induce the gel-to-sol transition caused by the disruption of intermolecular Pt···Pt and π ··· π stacking interactions. This study not only enriches the library of functionalized well-defined metallacycles with intriguing spectroscopic and luminescence properties, but also provides a new opportunity to prepare smart soft materials through hierarchical self-assembly.

Experimental Section

Synthesis of metallacycle A

The dipyridyl donor ligand **a** (17.78 mg, 12.0 μmol) and organoplatinum 180° acceptor **10** (12.76 mg, 12.0 μmol) were weighed accurately into a glass vial. Acetone (5.0 mL) and water (1.0 mL) were added to the vial. The reaction solution was then stirred at 55 °C for 15 h to yield a homogeneous orange solution. KPF_6 (excess) was then added to the bottle with continuous stirring (10 min) to precipitate the product. The reaction mixture was centrifuged, washed several times with water, and dried. Yellow product **A** (29.32 mg, 96%) was collected and redissolved in CD_2Cl_2 for NMR spectroscopy analysis. IR (neat): $\bar{\nu} = 2962, 2925, 2853, 2224, 2119, 1608, 1575, 1455, 1415, 1306, 1262, 1092, 1067, 1035, 833, 760, 732, 702 \text{ cm}^{-1}$; ^1H NMR (400 MHz; CD_2Cl_2): $\delta = 8.94$ (s, 4H), 8.65 (s, 4H), 8.58 (d, 4H, $J = 8.0 \text{ Hz}$), 8.40 (d, 4H, $J = 7.6 \text{ Hz}$), 8.10 (s, 2H), 7.71–7.82 (m, 16H), 7.55 (s, 4H), 7.43 (d, 4H, $J = 8.2 \text{ Hz}$), 7.27 (s, 4H), 7.08 (s, 4H), 4.59 (s, 8H), 4.36 (s, 4H), 1.93 (s, 12H), 1.18–1.54 (m, 228H), 0.83–0.87 ppm (m, 18H); ^{31}P NMR (CD_2Cl_2 , 161.9 MHz): $\delta = 13.38$ ppm (s, $J(\text{Pt},\text{P}) = 2724.1 \text{ Hz}$); ESI-TOF-MS: m/z calcd for $\text{C}_{214}\text{H}_{322}\text{F}_{12}\text{N}_{14}\text{O}_2\text{P}_{10}\text{Pt}_6$ [$M - 4\text{PF}_6$] $^{4+}$, $\text{C}_{214}\text{H}_{322}\text{F}_6\text{N}_{14}\text{O}_2\text{P}_9\text{Pt}_6$ [$M - 5\text{PF}_6$] $^{5+}$: 1207.2596, 936.8181; found: 1207.3376, 936.8266.

Synthesis of metallacycle B

By following the procedure reported for **A**, ligand **a** (11.30 mg, 7.6 μmol) and organoplatinum 180° acceptor **11** (8.69 mg, 7.6 μmol) yielded **B** as a yellow solid (19.59 mg, 98%). IR (neat): $\bar{\nu} = 2922, 2851, 2220, 2115, 1609, 1577, 1455, 1414, 1306, 1262, 1106, 1070, 1034, 837, 761 \text{ cm}^{-1}$; ^1H NMR (400 MHz; CD_2Cl_2): $\delta = 8.97$ (s, 4H), 8.65 (s, 4H), 8.60 (d, 4H, $J = 8.2 \text{ Hz}$), 8.38 (d, 4H, $J = 7.2 \text{ Hz}$), 8.14 (s, 2H), 7.43–7.81 (m, 40H), 4.61 (s, 8H), 4.37 (s, 4H), 1.94 (s, 12H), 1.19–1.57 (m, 228H), 0.83–0.87 ppm (m, 19H); ^{31}P NMR (CD_2Cl_2 , 161.9 MHz): $\delta = 13.97$ ppm (s, $J(\text{Pt},\text{P}) = 2677.8 \text{ Hz}$); ESI-TOF-MS: m/z calcd for $\text{C}_{226}\text{H}_{330}\text{F}_{12}\text{N}_{14}\text{O}_2\text{P}_{10}\text{Pt}_6$ [$M - 4\text{PF}_6$] $^{4+}$, $\text{C}_{226}\text{H}_{330}\text{F}_6\text{N}_{14}\text{O}_2\text{P}_9\text{Pt}_6$ [$M - 5\text{PF}_6$] $^{5+}$: 1245.2754, 967.2306; found: 1245.3689, 967.2462.

Synthesis of metallacycle C

By following the procedure reported for **A**, ligand **b** (12.95 mg, 8.7 μmol) and organoplatinum 180° acceptor **12** (10.17 mg, 8.7 μmol) yielded **C** as a yellow solid (22.20 mg, 96%). IR (neat): $\bar{\nu} = 2917, 2852, 2219, 2112, 1609, 1573, 1486, 1453, 1417, 1381, 1307, 1279, 1208, 1037, 835, 762 \text{ cm}^{-1}$; ^1H NMR (400 MHz; CD_2Cl_2): $\delta = 9.16$ (d, 4H, $J = 4.2 \text{ Hz}$), 8.84 (s, 8H), 8.51 (s, 4H), 8.17 (s, 4H), 7.54–8.01 (m, 34H), 7.38 (s, 4H), 4.55 (s, 8H), 4.32 (s, 4H), 1.91 (s, 12H), 1.19–1.44 (m, 228H), 0.82–0.86 ppm (m, 18H); ^{31}P NMR (CD_2Cl_2 ,

161.9 MHz): $\delta = 12.83$ ppm (*s*, $J(\text{Pt},\text{P}) = 2690.8$ Hz); ESI-TOF-MS: *m/z* calcd for $\text{C}_{230}\text{H}_{328}\text{F}_{12}\text{N}_{14}\text{O}_2\text{P}_{10}\text{Pt}_6$ [$M - 4\text{PF}_6$] $^{4+}$, $\text{C}_{230}\text{H}_{328}\text{F}_6\text{N}_{14}\text{O}_2\text{P}_9\text{Pt}_6$ [$M - 5\text{PF}_6$] $^{5+}$: 1257.0234, 976.8306; found: 1257.0801, 976.8008.

Acknowledgements

This study was financially supported by NSFC (China) (nos. 21322206 and 21132005) and the Key Basic Research Project of Shanghai Science and Technology Commission (no. 13JC1402200).

Keywords: gels • metallacycles • platinum • self-assembly • supramolecular chemistry

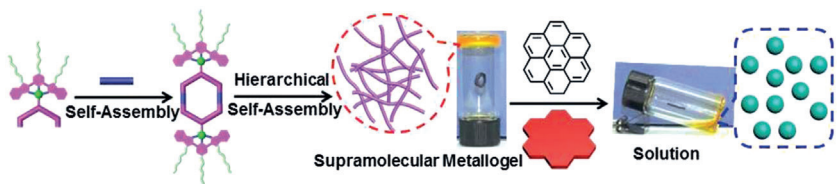
- [1] a) J.-M. Lehn, *Supramolecular Chemistry*, VCH, Weinheim, 1995; b) *Comprehensive Supramolecular Chemistry* (Eds.: J. L. Atwood, J. E. D. Davies, D. D. MacNicol, F. Vögtle), Pergamon, New York, 1996; c) J. W. Steed, J. L. Atwood, *Supramolecular Chemistry*, Wiley, New York, 2000.
- [2] a) J. Rebek, Jr., *Acc. Chem. Res.* **1999**, *32*, 278–286; b) J. Rebek, Jr., *Acc. Chem. Res.* **2009**, *42*, 1660–1668; c) F. J. M. Hoeben, P. Jonkheijm, E. W. Meijer, A. P. H. J. Schenning, *Chem. Rev.* **2005**, *105*, 1491–1546; d) T. F. A. De Greef, M. M. J. Smulders, M. Wolffs, A. P. H. J. Schenning, R. P. Sijbesma, E. W. Meijer, *Chem. Rev.* **2009**, *109*, 5687–5754; e) M.-X. Wang, *Acc. Chem. Res.* **2012**, *45*, 182–195; f) R. S. Forgan, J.-P. Sauvage, J. F. Stoddart, *Chem. Rev.* **2011**, *111*, 5434–5464; g) H. Yang, B. Yuan, X. Zhang, *Acc. Chem. Res.* **2014**, *47*, 2106–2115; h) C. J. Bruns, J. F. Stoddart, *Acc. Chem. Res.* **2014**, *47*, 2186–2199; i) S. Dong, B. Zheng, F. Wang, F. Huang, *Acc. Chem. Res.* **2014**, *47*, 1982–1994; j) J. D. Crowley, S. M. Goldup, A.-L. Lee, D. A. Leigh, R. T. McBurney, *Chem. Soc. Rev.* **2009**, *38*, 1530–1541; k) J.-F. Ayme, J. E. Beves, C. J. Campbell, D. A. Leigh, *Chem. Soc. Rev.* **2013**, *42*, 1700–1712.
- [3] a) S. Leininger, B. Olenyuk, P. J. Stang, *Chem. Rev.* **2000**, *100*, 853–908; b) S. R. Seidel, P. J. Stang, *Acc. Chem. Res.* **2002**, *35*, 972–983; c) R. Chakrabarty, P. S. Mukherjee, P. J. Stang, *Chem. Rev.* **2011**, *111*, 6810–6918; d) M. Fujita, *Acc. Chem. Res.* **1999**, *32*, 53–61; e) M. Fujita, M. Tominaga, A. Hori, B. Therrien, *Acc. Chem. Res.* **2005**, *38*, 371–380; f) M. D. Pluth, R. G. Bergman, K. N. Raymond, *Acc. Chem. Res.* **2009**, *42*, 1650–1659; g) C. G. Oliveri, P. A. Ulmann, M. J. Wiester, C. A. Mirkin, *Acc. Chem. Res.* **2008**, *41*, 1618–1629; h) J. R. Nitschke, *Acc. Chem. Res.* **2007**, *40*, 103–112; i) A. M. Castilla, W. J. Ramsay, J. R. Nitschke, *Acc. Chem. Res.* **2014**, *47*, 2063–2073; j) Y.-F. Han, W.-G. Jia, W.-B. Yu, G.-X. Jin, *Chem. Soc. Rev.* **2009**, *38*, 3419–3434; k) Y.-F. Han, G.-X. Jin, *Chem. Soc. Rev.* **2014**, *43*, 2799–2823; l) M. Yoshizawa, J. K. Klosterman, *Chem. Soc. Rev.* **2014**, *43*, 1885–1898; m) M. Han, D. M. Engelhard, G. H. Clever, *Chem. Soc. Rev.* **2014**, *43*, 1848–1860; n) S. H. A. M. Leenders, R. Gramage-Doria, B. Bruin, J. N. H. Reek, *Chem. Soc. Rev.* **2015**, *44*, 433–448; o) K. Baek, I. Hwang, I. Roy, D. Shetty, K. Kim, *Acc. Chem. Res.* **2015**, *48*, 2221–2229; p) S. Shanmugaraju, P. S. Mukherjee, *Chem. Eur. J.* **2015**, *21*, 6656–6666.
- [4] a) B. Olenyuk, J. A. Whiteford, A. Fechtenkötter, P. J. Stang, *Nature* **1999**, *398*, 796–799; b) Q.-F. Sun, J. Iwasa, D. Ogawa, Y. Ishido, S. Sato, T. Ozeki, Y. Sei, K. Yamaguchi, M. Fujita, *Science* **2010**, *328*, 1144–1147; c) P. Mal, B. Breiner, K. Rissanen, J. R. Nitschke, *Science* **2009**, *324*, 1697–1699; d) G. H. Clever, W. Kawamura, S. Tashiro, M. Shiro, M. Shionoya, *Angew. Chem. Int. Ed.* **2012**, *51*, 2606–2609; *Angew. Chem.* **2012**, *124*, 2660–2663; e) M. Han, R. Michel, B. He, Y.-S. Chen, D. Stalke, M. John, G. H. Clever, *Angew. Chem. Int. Ed.* **2013**, *52*, 1319–1323; *Angew. Chem.* **2013**, *125*, 1358–1362; f) N. Kishi, M. Akita, M. Yoshizawa, *Angew. Chem. Int. Ed.* **2014**, *53*, 3604–3607; *Angew. Chem.* **2014**, *126*, 3678–3681; g) B. Roy, A. K. Ghosh, S. Srivastava, P. D'Silva, P. S. Mukherjee, *J. Am. Chem. Soc.* **2015**, *137*, 11916–11919; h) P. Howlader, P. Das, E. Zangrando, P. S. Mukherjee, *J. Am. Chem. Soc.* **2016**, *138*, 1668–1676; i) M. Wang, C. Wang, X.-Q. Hao, J. Liu, X. Li, C. Xu, A. Lopez, L. Sun, M.-P. Song, H.-B. Yang, X. Li, *J. Am. Chem. Soc.* **2014**, *136*, 6664–6671; j) M. Wang, C. Wang, X.-Q. Hao, X. Li, T. J. Vaughn, Y.-Y. Zhang, Y. Yu, Z.-Y. Li, M.-P. Song, H.-B. Yang, X. Li, *J. Am. Chem. Soc.* **2014**, *136*, 10499–10507.
- [5] a) M. Yoshizawa, M. Tamura, M. Fujita, *Science* **2006**, *312*, 251–254; b) M. D. Pluth, R. G. Bergman, K. N. Raymond, *Science* **2007**, *316*, 85–88;
- [6] a) C. Zhao, Q.-F. Sun, W. M. Hart-Cooper, A. G. DiPasquale, F. D. Toste, R. G. Bergman, K. N. Raymond, *J. Am. Chem. Soc.* **2013**, *135*, 18802–18805; b) C. Zhao, F. D. Toste, K. R. Raymond, R. G. Bergman, *J. Am. Chem. Soc.* **2014**, *136*, 14409–14412; c) K. Harano, S. Hiraoka, M. Shiohonya, *J. Am. Chem. Soc.* **2007**, *129*, 5300–5301; f) X.-F. Jiang, F. K.-W. Hau, Q.-F. Sun, S.-Y. Yu, V. W.-W. Yam, *J. Am. Chem. Soc.* **2014**, *136*, 10921–10929; g) X. Yan, T. R. Cook, P. Wang, F. Huang, P. J. Stang, *Nat. Chem.* **2015**, *7*, 342–348; h) A. Chowdhury, P. Howlader, P. S. Mukherjee, *Chem. Eur. J.* **2016**, *22*, 7468–7478.
- [7] a) T. R. Cook, Y.-R. Zheng, P. J. Stang, *Chem. Rev.* **2013**, *113*, 734–777; b) L. Xu, L.-J. Chen, H.-B. Yang, *Chem. Commun.* **2014**, *50*, 5156–5170; c) M. Yoshizawa, J. K. Klosterman, M. Fujita, *Angew. Chem. Int. Ed.* **2009**, *48*, 3418–3438; *Angew. Chem.* **2009**, *121*, 3470–3490; d) K. Harris, D. Fujita, M. Fujita, *Chem. Commun.* **2013**, *49*, 6703–6712; e) A. J. McConnell, C. S. Wood, P. P. Neelakandan, J. R. Nitschke, *Chem. Rev.* **2015**, *115*, 7729–7793; f) L. Xu, Y.-X. Wang, L.-J. Chen, H.-B. Yang, *Chem. Soc. Rev.* **2015**, *44*, 2148–2167; g) W. Wang, Y.-X. Wang, H.-B. Yang, *Chem. Soc. Rev.* **2016**, *45*, 2656–2693.
- [8] a) S. Chen, L.-J. Chen, H.-B. Yang, H. Tian, W. Zhu, *J. Am. Chem. Soc.* **2012**, *134*, 13596–13599; b) J.-K. Ou-Yang, Y.-Y. Zhang, M.-L. He, J.-T. Li, X. Li, X.-L. Zhao, C.-H. Wang, Y. Yu, D.-X. Wang, L. Xu, H.-B. Yang, *Org. Lett.* **2014**, *16*, 664–667; c) X.-D. Xu, C.-J. Yao, L.-J. Chen, G.-Q. Yin, Y.-W. Zhong, H.-B. Yang, *Chem. Eur. J.* **2016**, *22*, 5211–5218; d) W. Wang, B. Sun, X.-Q. Wang, Y.-Y. Ren, L.-J. Chen, J. Ma, Y. Zhang, X. Li, Y. Yu, H. Tan, H.-B. Yang, *Chem. Eur. J.* **2015**, *21*, 6286–6294.
- [9] a) Z.-Y. Li, Y. Zhang, C.-W. Zhang, L.-J. Chen, C. Wang, H. Tan, Y. Yu, X. Li, H.-B. Yang, *J. Am. Chem. Soc.* **2014**, *136*, 8577–8589; b) L.-J. Chen, G.-Z. Zhao, B. Jiang, B. Sun, M. Wang, L. Xu, J. He, Z. Abliz, H. Tan, X. Li, H.-B. Yang, *J. Am. Chem. Soc.* **2014**, *136*, 5993–6001; c) G.-Z. Zhao, L.-J. Chen, W. Wang, J. Zhang, G. Yang, D.-X. Wang, Y. Yu, H.-B. Yang, *Chem. Eur. J.* **2013**, *19*, 10094–10100; d) N.-W. Wu, L.-J. Chen, C. Wang, Y.-Y. Ren, X. Li, L. Xu, H.-B. Yang, *Chem. Commun.* **2014**, *50*, 4231–4233; e) L.-J. Chen, Y.-Y. Ren, N.-W. Wu, B. Sun, J.-Q. Ma, L. Zhang, H. Tan, M. Liu, X. Li, H.-B. Yang, *J. Am. Chem. Soc.* **2015**, *137*, 11725–11735.
- [10] a) V. W.-W. Yam, V. K.-M. Au, S. Y.-L. Leung, *Chem. Rev.* **2015**, *115*, 7589–7728; b) K. M.-C. Wong, V. W.-W. Yam, *Acc. Chem. Res.* **2011**, *44*, 424–434; c) M. Mauro, A. Aliprandi, D. Septiadi, N. S. Kehr, L. D. Cola, *Chem. Soc. Rev.* **2014**, *43*, 4144–4166; d) A. N. Vedernikov, *Acc. Chem. Res.* **2012**, *45*, 803–813; e) I. Eryazici, C. N. Moorefield, G. R. Newkome, *Chem. Rev.* **2008**, *108*, 1834–1895.
- [11] a) A. K.-W. Chan, W. H. Lam, Y. Tanaka, K. M.-C. Wong, V. W.-W. Yam, *Proc. Natl. Acad. Sci. USA* **2015**, *112*, 690–695; b) C. Y.-S. Chung, V. W.-W. Yam, *J. Am. Chem. Soc.* **2011**, *133*, 18775–18784; c) A. Aliprandi, M. Mauro, L. D. Cola, *Nat. Chem.* **2016**, *8*, 10–15; d) C. A. Strassert, C.-H. Chien, M. D. G. Lopez, D. Kourkoulos, D. Hertel, K. Meerholz, L. D. Cola, *Angew. Chem. Int. Ed.* **2011**, *50*, 946–950; *Angew. Chem.* **2011**, *123*, 976–980; e) T. Zou, J. Liu, C. T. Lum, C. Ma, R. C.-T. Cahn, C.-N. Lok, W.-M. Kwok, C.-M. Che, *Angew. Chem. Int. Ed.* **2014**, *53*, 10119–10123; *Angew. Chem.* **2014**, *126*, 10283–10287; f) S. C. F. Kui, S. S.-Y. Chui, C.-M. Che, N. Zhu, *J. Am. Chem. Soc.* **2006**, *128*, 8297–8309.
- [12] a) T. Tu, W. Fang, X. Bao, X. Li, K. H. Dötz, *Angew. Chem. Int. Ed.* **2011**, *50*, 6601–6605; *Angew. Chem.* **2011**, *123*, 6731–6735; b) L.-B. Xing, S. Yu, X.-J. Wang, G.-X. Wang, B. Chen, L.-P. Zhang, C.-H. Tung, L.-Z. Wu, *Chem. Commun.* **2012**, *48*, 10886–10888; c) L.-B. Xing, X.-J. Wang, X.-W. Gao, B. Chen, C.-H. Tung, L.-Z. Wu, *Supramol. Chem.* **2015**, *27*, 298–302; d) F. Camerel, R. Ziessl, B. Donnio, C. Bourgogne, D. Guillon, M. Schmutz, C. Iacobita, J.-P. Bucher, *Angew. Chem. Int. Ed.* **2007**, *46*, 2659–2662; *Angew. Chem.* **2007**, *119*, 2713–2716; e) L. J. Grove, J. M. Rennekkamp, H. Jude, W. B. Connick, *J. Am. Chem. Soc.* **2004**, *126*, 1594–1595; f) T. J. Wadas, Q.-M. Wang, Y. Kim, C. Flaschenreim, T. N. Blanton, R. Eisenberg, *J. Am. Chem. Soc.* **2004**, *126*, 16841–16849.
- [13] a) A. Y.-Y. Tam, W. H. Lam, K. M.-C. Wong, N. Zhu, V. W.-W. Yam, *Chem. Eur. J.* **2008**, *14*, 4562–4576; b) A. Y.-Y. Tam, K. M.-C. Wong, V. W.-W. Yam, *J. Am. Chem. Soc.* **2009**, *131*, 6253–6260; c) C. Po, A. Y.-Y. Tam, K. M.-C. Wong, V. W.-W. Yam, *J. Am. Chem. Soc.* **2011**, *133*, 12136–12143; d) C. Po, A. Y.-Y. Tam, V. W.-W. Yam, *Chem. Sci.* **2014**, *5*, 2688–2695; e) C. Po, V. W.-W. Yam, *Chem. Sci.* **2014**, *5*, 4868–4872.
- [14] a) B. Jiang, J. Zhang, J.-Q. Ma, W. Zheng, L.-J. Chen, B. Sun, C. Li, B.-W. Hu, H. Tan, X. Li, H.-B. Yang, *J. Am. Chem. Soc.* **2016**, *138*, 738–741.
- [15] a) P. Spenst, F. Würthner, *Angew. Chem. Int. Ed.* **2015**, *54*, 10165–10168; *Angew. Chem.* **2015**, *127*, 10303–10306; b) J. C. Barnes, M. Juríček, N. L.

- Strutt, M. Frasconi, S. Sampath, M. A. Giesener, P. L. McGrier, G. J. Bruns, C. L. Stern, A. A. Sarjeant, J. F. Stoddart, *J. Am. Chem. Soc.* **2013**, *135*, 183–192; c) K. Omoto, S. Tashiro, M. Kuritani, M. Shionoya, *J. Am. Chem. Soc.* **2014**, *136*, 17946–17949; d) K. Saigo, R.-J. Lin, M. Kubo, A. Youda, M. Hasegawa, *J. Am. Chem. Soc.* **1986**, *108*, 1996–2000; e) Y. Tanaka, K. M.-C. Wong, V. W.-W. Yam, *Chem. Eur. J.* **2013**, *19*, 390–399.
- [15] a) J. W. Steed, *Chem. Soc. Rev.* **2010**, *39*, 3686–3699; b) D. K. Kumar, J. W. Steed, *Chem. Soc. Rev.* **2014**, *43*, 2080–2088; c) L. Meazza, J. A. Foster, K. Fucke, P. Metrangolo, G. Resnati, J. W. Steed, *Nat. Chem.* **2013**, *5*, 42–47.
- [16] a) W. Fang, C. Liu, J. Chen, Z. Lu, Z.-M. Li, X. Bao, T. Tu, *Chem. Commun.* **2015**, *51*, 4267–4270; b) W. Fang, C. Liu, Z. Liu, Z. Sun, T. Tu, *Chem. Commun.* **2014**, *50*, 10118–10121; c) W. Fang, X. Liu, Z. Lu, T. Tu, *Chem. Commun.* **2014**, *50*, 3313–3316.

Received: April 11, 2016

Published online on ■■■, 0000

FULL PAPER



Guest-induced behavior changes: A novel alkynylplatinum(II) 2,6-bis(benzoimidazol-2'-yl)pyridine (bzimpy)-functionalized supramolecular metallacycle was able to hierarchically self-assemble into an aromatic guest stimuli-responsive

metallogel at room temperature, without the need for a heating–cooling process, mainly driven by intermolecular Pt…Pt and π–π stacking interactions (see figure).

Supramolecular Chemistry

B. Jiang, J. Zhang, W. Zheng, L.-J. Chen,
G.-Q. Yin, Y.-X. Wang, B. Sun, X. Li,
H.-B. Yang*

■ ■ – ■ ■

Construction of Alkynylplatinum(II) Bzimpy-Functionalized Metallacycles and Their Hierarchical Self-Assembly Behavior in Solution Promoted by Pt…Pt and π–π Interactions

